Stochastic Modeling of 2D Photonic Crystals

Mohamed I. Wafa
Cairo University Faculty of Engineering
Yasser M. El-Batawy (ymbatawy@gmail.com)
Cairo University - Faculty of Engineering https://orcid.org/0000-0002-2960-8808
Sahar A. El-Naggar
Cairo University Faculty of Engineering

Research Article

Keywords: Two Dimensional Photonic Crystals, stochastic modeling, Monte Carlo, photonic Bandgap, fabrication uncertainty

Posted Date: February 18th, 2021

DOI: https://doi.org/10.21203/rs.3.rs-203814/v1

Stochastic Modeling of 2D Photonic Crystals

Mohamed I. Wafa [a,b], Yasser M. El-Batawy [a,b], Sahar A. El-Naggar [a]

[(a)] Department of Engineering Math and Physics, Faculty of Engineering, Cairo University, 12613 Giza, Egypt

[(b)] Nanoelectronics Integrated Systems Center, Nile University, 12588 Giza, Egypt

Abstract

Due to the fabrication processes, inaccurate manufacturing of the photonic crystals (PCs) might occur which affect their performance. In this paper, we examine the effects of tolerance variations of the radii of the rods and the permittivity of the material of the two-dimensional PCs on their performance. The presented stochastic analysis relies on plane wave expansion method and Mote Carlo simulations. We focus on two structures, namely Si-Rods PCs and Air-Holes PCs. Numerical results show – for both structures – that uncertainties in the dimensions of the PCs have higher impact on its photonic gap than do the uncertainties in the permittivity of the Si material. In addition, Air-Holes PCs could be a good candidate with least alteration in the photonic gap considering deviations that might occur in the permittivity of Si due to impurities up to 5%.

Keywords: *Two Dimensional Photonic Crystals, stochastic modeling, Monte Carlo, photonic Bandgap, fabrication uncertainty*

1. Introduction

Photonic Crystals (PCs) are promising candidates for many applications, and they might act as a waveguide or microcavity laser [1,2] because PCs are engineered to provide controlled optical properties. Such optical properties are not available in homogeneous materials. It is known that PCs are designed to have a periodic structure of different materials which can control the electromagnetic waves propagation through the photonic crystal [3]. The structures of the PCs exhibit a photonic bandgap (PBG), where the electromagnetic wave cannot propagate in this range of frequencies due to the total reflection [4]. In many applications, a large PBG of PCs is considered as an important feature [5]. The PCs' designs and fabrications are challenging due to the diversity of periodic arrangement and layer dimensions and

materials which the designed PC needs. For two-dimensional PCs, the embedding of circular rods into square array and changing the radius of one or more rods results in defect modes. In [6], varying of an air-rod radius that is placed at the center of the array leads to local defects with tunable frequencies those depend on the radius of these air rods.

The widely used fabrication approaches of photonic crystals are mainly microfabrication etching or thin film fabrication [7]. In these fabrication processes, it is too difficult for exact realization of dimensions of the photonic crystal and the permittivities of its materials. This fabrication inaccuracies affect the operating performance of the PCs. In the presented work, we investigate the effects of deviations – that may arise due to fabrication issues – in the photonic crystals' components on their photonic band gap. We consider deviations that might occur in the dimensions as well as the permittivity of the PC's material using Monte Carlo simulation.

We have applied Monte Carlo technique for the stochastic analysis part in this work because it is widely used technique to determine tolerance [8,9]. In addition, Monte Carlo modeling is accurate, and easy to implement approach. In [8], Monte Carlo modeling of imperfections in the materials of 2D-PCs is applied. In [9], a multiscale continuous Galerkin method has been used providing high accuracy and fact stochastic simulation of time-harmonic wave propagation through PCs. The technique is used in [10] to study the properties of photonic band gaps in 2D plasma-dielectric PCs using the modified plane wave expansion method. Monte Carlo has been used [11] to investigate the impacts of the randomness on the optical featured of waveguides embedded in disordered 2D-PCs for TM-polarized radiation. In our previous work [12], a stochastic analysis of one dimensional PC has been studied showing the impacts of the tolerances in PC's dimensions on the operating optical properties for defect free PC and for PC with a defect air-layer.

In this work, we consider two types of 2D Photonic Crystals; the first type has rods with high refractive index placed in background of lower refractive index, whereas the second type is constructed of rods with lower refractive index compared to the background of the crystal. For these structures, we focus our attention on the stochastic analysis of 2D-PCs where the effects of the tolerances of both the dimensions of the PC and permittivities of its materials on the normalized gap-width are modeled and studied. In this stochastic analysis, the effects of the uncertainties of the radii of the rods and the lattice constant of the crystal on its functionality are considered. We have also studied the effects of stochastic

changes that might occur in the relative permittivity of the PC rods that may results from the impurities. Our work is based on the plane wave expansion and Monte Carlo simulation. Our results revealed that the uncertainties in the dimensions of the PCs have serious consequences on the photonic gap than do the uncertainties in the permittivity of the Si material.

First, the proposed 2D-PCs structures are detailed described and the presented stochastic modeling is presented and discussed in section 2. After that, the numerical results of the stochastic analyses are presented in section 3, where both 2D-PCs with Si rods in air background and 2D-PCs with air-Holes in Si background are studied. In both structures, the impacts of the tolerances in the crystal dimensions and permittivities on the operating photonic bandgap are investigated. Finally, the conclusions are summarized.

2. Stochastic Modeling and Methods

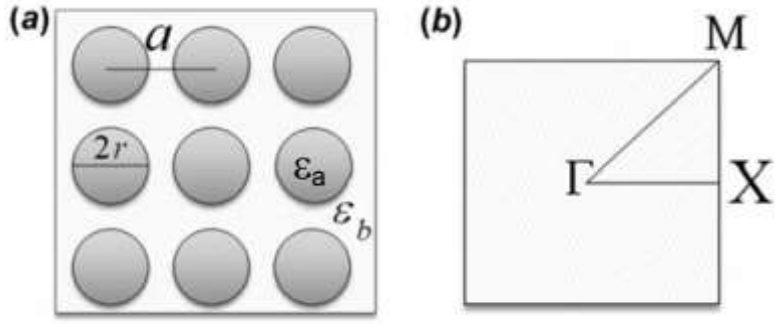

Figure 1: (a) Cross-section of 2D PCs with rods with relative permittivity of ε_a embedded into a square lattice of background with relative permittivity of ε_b, (b) First Brillouin zone of the square lattice.

Figure 1 shows a schematic of 2D photonic crystal where the rods (of radius *r*) are embedded into the background of square lattice with a lattice spacing of *a*. The rods of 2D-PC are parallel having length much greater than *r* and these rods are placed along the *z*-direction. The relative permittivities of the rods

and the background are ε_a and ε_b, respectively. In the presented modeling, transverse-electric field (TE) is considered. It is defined as:

$$E(r,t) = E_z(r)e^{-i\,\omega t}, \qquad (1)$$

where ω and r are the angular frequency and , respectively. For TE, both the dielectric function and the electric field can be expanded in a Fourier series due to the periodicity in the x-y plane, resulting in the following eigenvalue problem,

$$(\mathbf{k}+\mathbf{G})^2 E_z(\mathbf{G}) = \frac{w^2}{c^2}\sum_{\mathbf{G}'}\varepsilon(\mathbf{G}-\mathbf{G}')E_z(\mathbf{G}'), \qquad (2)$$

where **k** and **G** are the two dimensional direct and reciprocal-lattice vectors. Equation (1) is solved numerically by substituting $\mathrm{G} = \left(\frac{2\pi}{a}\right)(n_1, n_2)$ for the square lattice where n_1 and n_2 are integers and the upper limit for both n_1 and n_2 is set to be ten, while the total number of plane waves of 441 are used which ensures adequate convergence [13,14]. In the presented numerical simulations, a normalized frequency of $\omega a/2\pi c = 1$ has been used and we have mainly focused on the normalized bandgap-width ($\Delta\omega/\omega_g$), where $\Delta\omega$ is the frequency of the photonic bandgap that results between the first and the second bands, and ω_g is at the middle of this frequency range.

In the presented stochastic model, Monte Carlo technique use the deterministic simulation code as a black-box that relates between inputs which express the design parameters of the 2D-PCs and the associated outputs those express the operating performance. The technique generates a large number of samples (M) and evaluates the deterministic model for each of them, resulting in the response vector. According to the law of large numbers, $\bar{x}$ and σ are defined as the mean and the standard deviation of these samples, respectively and they can be determined as following:

$$\bar{x} \approx \frac{\sum_{i=1}^{M} x_i}{M}, \qquad (3)$$

$$\sigma \approx \sqrt{\frac{M}{M-1}\left[\frac{\sum_{i=1}^{M} x_i^2}{M} - \bar{x}^2\right]}. \qquad (4)$$

It is worth mentioning that increasing the number of samples enhances the degree of accuracy of the probability distribution function PDF of the output response and leads to a decrease in the standard deviation σ.

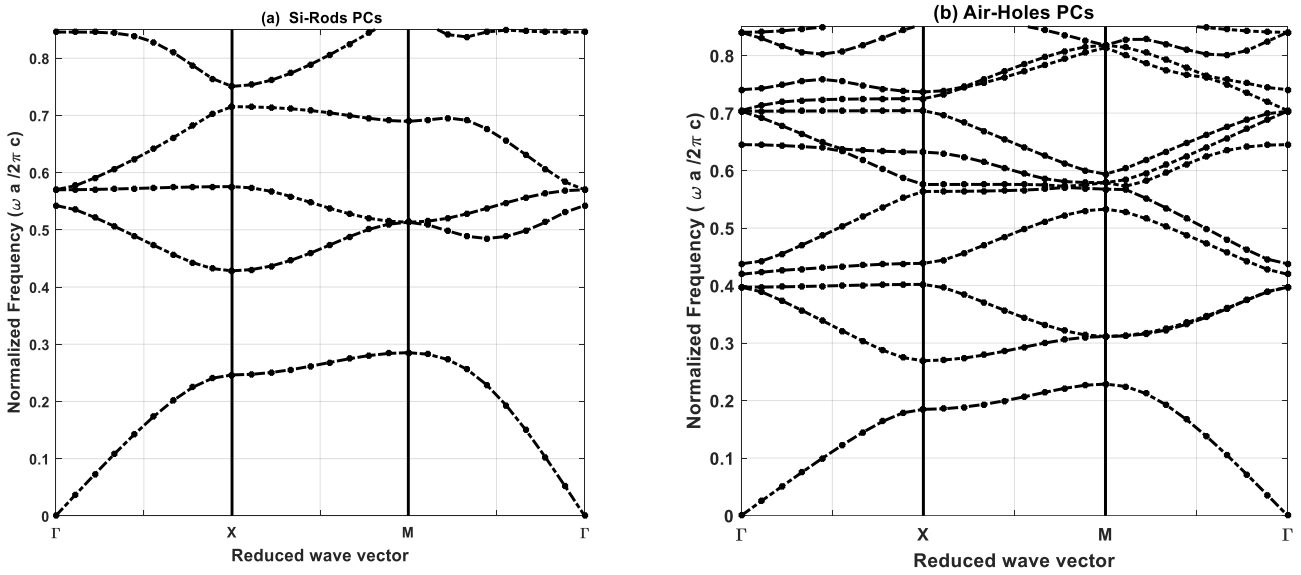

Figure 2: The photonic band structure for (a) Si-Rods PCs and (b) Air-Holes PCs.

3. Modeling Results

In these simulations, we consider two types of 2D photonic crystals (2D-PCs). The first type is composed of Si rods embedded in air background and we refer to this type as Si-Rods PCs. In this type, we set r/a=0.2, ε_a=12.4 and ε_b=1. The second type of the studied 2D-PCs is composed of air holes in a Si background and we refer to this type as Air-Holes PCs. In this type, we set r/a =0.45, ε_a=1 and ε_b=12.4. In order to held comparison between photonic band gaps of the two structures, we calculate the normalized photonic bandgap ($\Delta\omega/\omega_g$), where $\Delta\omega$ is the frequency of the bandgap width that results between the first and second band and ω_g is the central frequency of the bandgap. The design parameters of the 2D-PC are r, a and ε_a and ε_b. The photonic bands of these 2D-PCs are shown in figure 2, and they are denoted by "deterministic case" where there is no uncertainty either in the dimensions or in the permittivities of the photonic crystals' materials.

In figure 2-a, the photonic band gap of Si-Rods PCs is shown where it extends from 0.2853 to 0.4283 in units of $2\pi c/a$, which gives $\Delta\omega/\omega_g = 40.08\%$. The photonic band gap of Air-Holes PCs structure is shown in figure 2-b, where it extends from 0.2287 to 0.2693 in units of $2\pi c/a$, which gives $\Delta\omega/\omega_g = 16.31\%$. In the following sections, we introduce uncertainty in our design parameters; namely r, a and ε of the Silicon

and examine the effects of these uncertainties on the normalized photonic band gap $\Delta\omega/\omega_g$ for each structure.

3.1 Si-Rods 2D-PCs

First, we consider uncertainties in both *a* and *r* by applying Monte Carlo technique with 10000 sample set size. In Figure 3, the photonic band gap is shown for uncertainties of 1%, 2%, 5% and 10% in both *a* and *r*, respectively. As shown in this figure, there is a large tolerance of the photonic bandgap width and its upper and lower limits. Also, the uncertainty of the bandgap width increases by increasing the tolerances of the rod radius and the lattice constant. The proven gap between the first and the second frequency bands for all given uncertainties of the PC stochastic parameters is defined as confident photonic bandgap [12]. The confident PBG is simulated for different uncertainties of both *r* and *a* and listed in Table 1, where it can be noticed easily that increasing these tolerances leads to a decrease of the width of the confident bandgap. Further increase in the uncertainties of the stochastic parameters of 2D-PC makes the confident bandgap disappears completely as in the case of 10% tolerance. In such case, the PC might not work as designed and losses its major feature.

Table 1: The confident PBG for different tolerances of *r* and *a*

Tolerance	Highest Normalized frequency of the first band	Lowest Normalized frequency of the second band	Confident $\Delta\omega$	Confident $\Delta\omega/\omega_g$
1%	0.2935	0.4169	0.1234	34.59%
2%	0.3023	0.4056	0.1033	28.95%
5%	0.3309	0.3761	0.0452	12.67%
10%	0.3893	0.3382	No Confident gap	0%

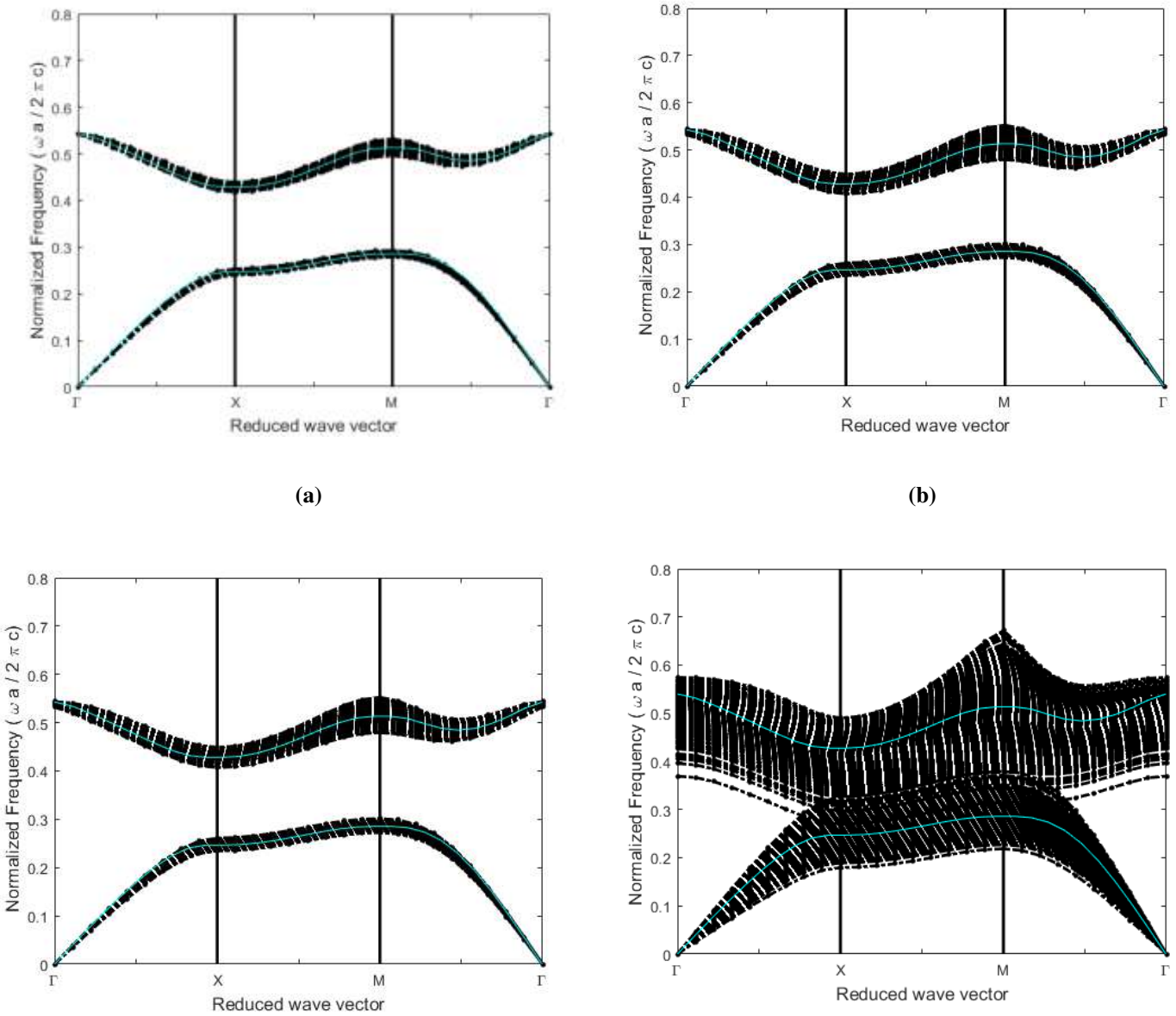

(a) **(b)**

(c) (d)

Figure 3: The Normalized frequency and Normalized frequency mean for tolerances of *r* and *a* of (a) 1%, (b) 2%, (c) 5% and (d) 10%.

We also plot mean and the standard deviation of the upper and the lower normalized frequencies for the band structure of the first PBG in Figure 4. As shown in these figures, by increasing the uncertainties in both *a* and *r*, the mean of the upper and the lower normalized frequencies of this band structure mainly are not affected by the uncertainties in these design parameters while the standard deviations increases

clearly by increasing these uncertainties as shown in Figure 4-b. The probability distribution function (PDF) of the normalized band gap for different tolerances are plotted in Figure 5(a) while the PDF of the normalized first and second bands for these tolerances are shown in Figure 5 (b). As shown in these figures, when the uncertainties in *a* and *r* increases from 1% to 10%, the PDF of the normalized bandgap extends over wider range, while the mean of the normalized frequency gap slightly changes. Also, the PDF of the normalized first and second bands broaden for larger uncertainties. The extension of the PDF over wide range reflects the increase in the standard deviation as well as the high uncertainty of both the bandgap width and its upper and lower edges.

The standard deviations σ for the PBGs for various uncertainties of *r* and *a* are shown in Table 2. In this table, it can be easily noted that the standard deviation increases more than 12 times as the uncertainty increases from 1% to 10%. In addition, the ratio between the standard deviation and the mean value of normalized band gap (σ/Mean) increases considerably with the increase of the uncertainties of *r* and *a* of the presented 2D-PC.

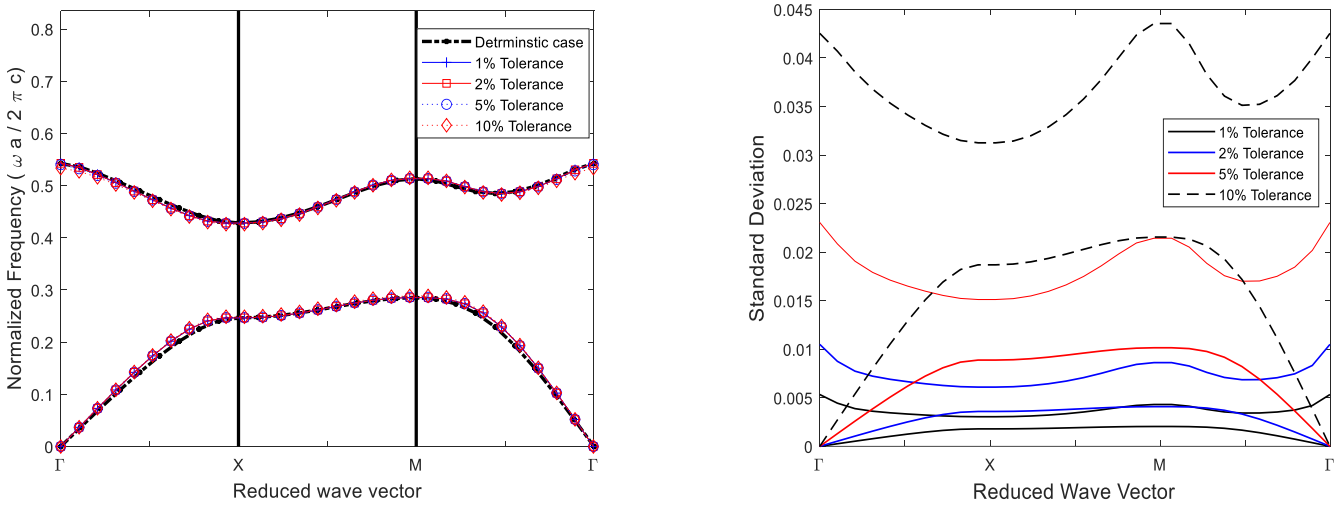

(a) **(b)**

Figure 4: (a) Mean value of the band structure and the PBG vs the reduced wave vector for tolerances of 1%, 2%, 5% and 10% in both *r* and *a*. (b) Standard Deviations of both lower and upper bands of the PBG for tolerances of 1%, 2%. 5% and 10% in both *r* and *a*.

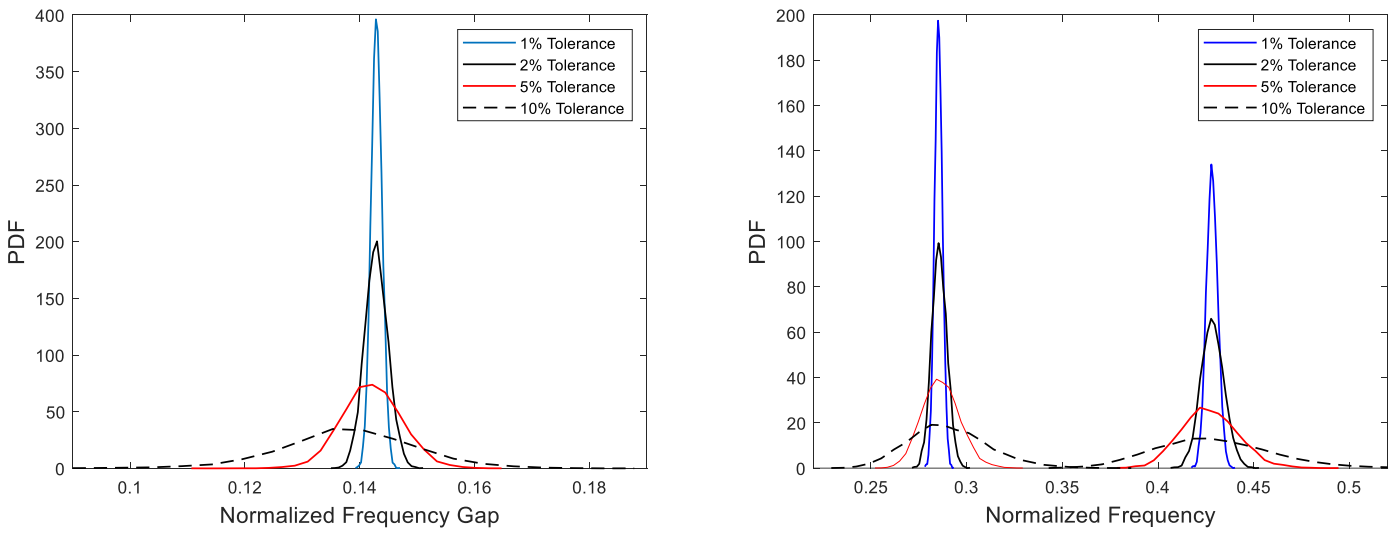

(a) **(b)**

Figure 5: (a) PDF of the normalized frequency of the bandgap width for different tolerances of *r* and *a* (b) PDF of The highest normalized frequency for the first band and the lowest Normalized frequency for the second band for different tolerances of *r* and *a*

Table 2: Mean and standard deviation of the normalized bandgap for different uncertainties of *r* and *a*

Tolerance	Mean of the highest Normalized frequency of the first band	Mean of the lowest Normalized frequency of the second band	Mean of PBG	Standard deviation of PBG	(σ/Mean) %
1%	0.2853	0.4283	0.1429	0.0010	0.7%
2%	0.2854	0.4282	0.1428	0.0020	1.4%
5%	0.2860	0.4276	0.1416	0.0054	3.8%
10%	0.2885	0.4260	0.1376	0.0126	9.15%

Next, the effects of the impurities of the material of rods of the Si-Rods PCs on its performance have been investigated. We consider uncertainties of 1%, 2% and 5% in the rod's permittivity ε_a and we plot the PDF of the bandgap and that of the first and second band frequency limits as shown in **Figure 6** (a) and (b), respectively. The standard deviations for the PBGs for various uncertainties of the permittivity

are shown in Table 3. We observe that the effects of the uncertainties in the permittivity on the band gap of the crystal are small compared to the case when considering the uncertainties of the crystal dimensions. In table 3, we note that increasing the tolerance from 1% to 5% leads to a change in σ/Mean ratio from 0.326% to 1.61%, while corresponding values in table 2 vary from 0.7% to 3.8%. We note from these percentages that the impact on σ/Mean due to deviations in the dimensions – r and a – is almost double its value due to deviations in the permittivity up to 5%.

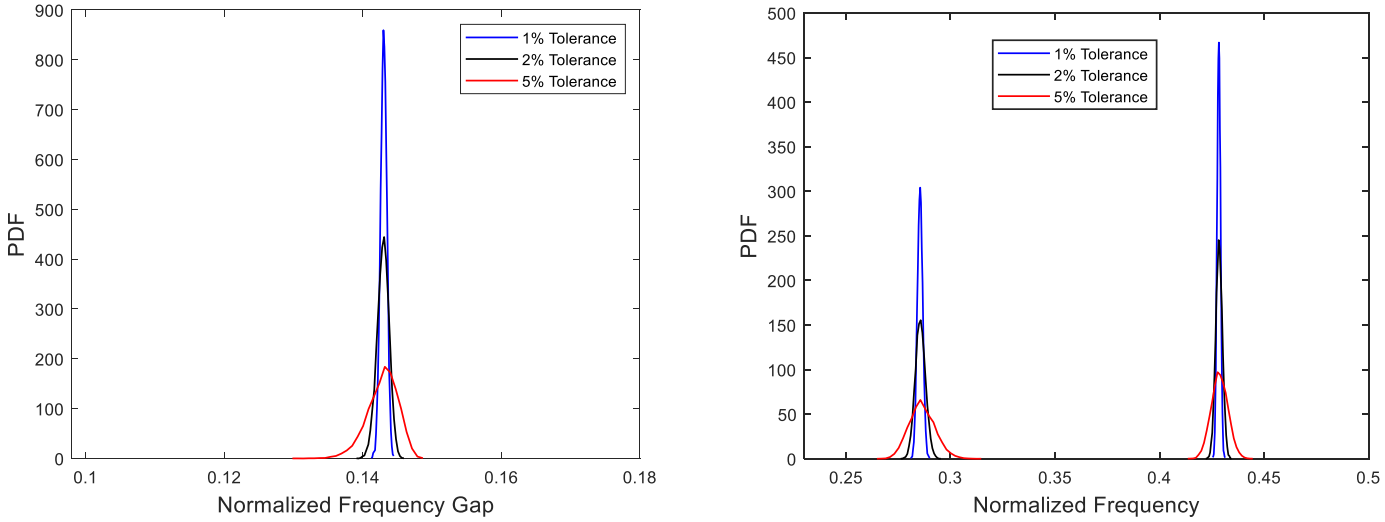

(a) **(b)**

Figure 6: (a) PDF of the normalized frequency gap for different tolerances of ε_a (b) PDF of The highest normalized frequency for the first band and the lowest Normalized frequency for the second band for different tolerances of ε_a

Table 3: Mean and standard deviation of the normalized bandgap for different uncertainties of rod's permittivity of the Si-Rods 2D-PCs structure

Tolerance	Mean of the highest Normalized frequency of the first band	Mean of the lowest Normalized frequency of the second band	Mean of PBG	Standard deviation of PBG	(σ/Mean) %
1%	0.2853	0.4283	0.1430	4.6657e-4	0.326%
2%	0.2853	0.4283	0.1430	9.1933e-4	0.642%
5%	0.2855	0.4283	0.1428	0.0023	1.61%

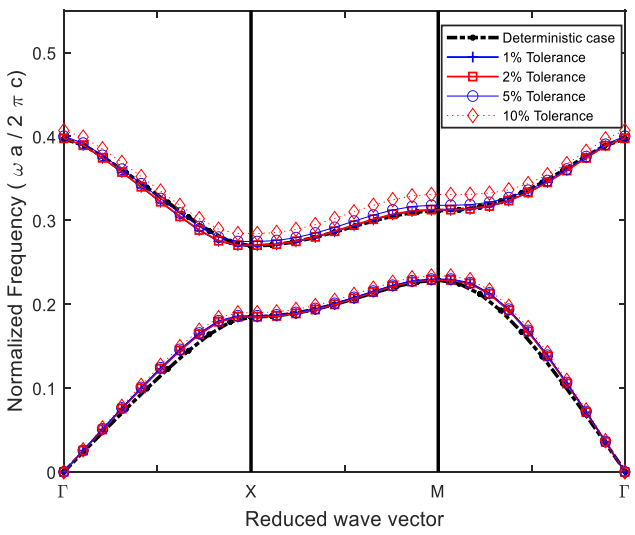

(a)

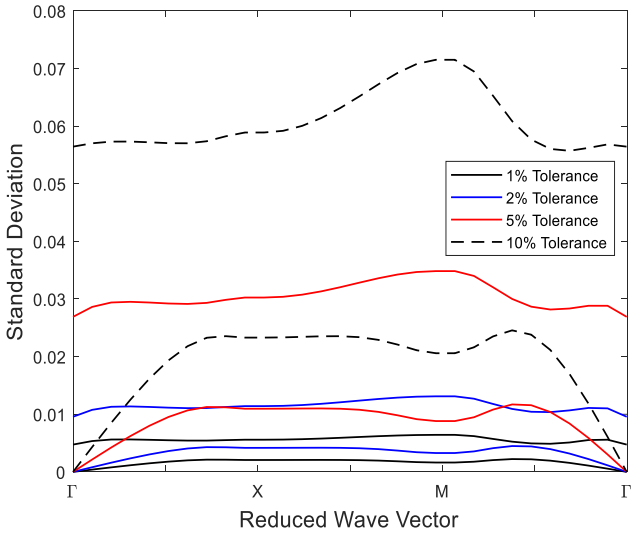

(b)

Figure 7: (a) The Mean value of the band structure and the PBG vs the reduced wave vector for tolerances of 1%, 2%, 5% and 10% in r. (b) Standard deviation of both the lower and upper bands of the PBG for tolerances of 1%, 2%. 5% and 10% in r.

3.2 Air-Holes 2D-PCs

In this section, we examine the effects of tolerances of the 2D-PC's stochastic parameters on the PBG in the case of Air-Holes 2D-PC's structure. The presented analysis starts by considering uncertainties of 1%, 2%, 5% and 10% in *r*. The mean of the lower and upper bands are plotted in Figure 7(a) for these values in addition to the deterministic case while the standard deviation of both the lower and the upper normalized frequencies for the band structure of the first PBG are shown in Figure 7(b). As shown in these figures, by increasing the tolerances in *r*, the mean of the upper and the lower normalized frequencies of this band structure mainly are not affected by the uncertainties in *r*. However, the standard deviations for these frequencies shown in Figure 7 (b) increase by increasing the tolerance from 1% to 10%. The standard deviations for the PBGs for various uncertainties of *r* are shown in Table 4. Comparison between Table 2 and Table 4 reveals that the standard deviations in Air-Holes PCs structure have much higher corresponding values for Si-Rods PCs structure. After that, the confident PBG width for different uncertainties of *r* for this PC structure have been evaluated and listed in Table 5. As shown

in this table, the normalized confident PBG $\Delta\omega/\omega_g$ decreases to 6.59% for a tolerance 1% in *r* while no confident gap is guaranteed for any further increase in this tolerance because the standard deviation is very high in this case.

Table 4 : Mean and standard deviation of the normalized bandgap for different uncertainties of *r*

Tolerance	Mean of the highest Normalized frequency of the first band	Mean of the lowest Normalized frequency of the second band	Mean of PBG	Standard deviation of PBG	(σ/Mean) %
1%	0.2288	0.2696	0.0409	0.0040	9.78%
2%	0.2289	0.2704	0.0415	0.0081	19.52%
5%	0.2299	0.2747	0.0448	0.0215	47.99%
10%	0.2337	0.2842	0.0506	0.0392	77.47%

Table 5: The confident PBG for different tolerances of *r*

Tolerance	Highest Normalized frequency of the first band	Lowest Normalized frequency of the second band	Confident $\Delta\omega$	Confident $\Delta\omega/\omega_g$
1%	0.2352	0.2516	0.0164	6.59%
2%	0.2460	0.2356	No Confident gap	0%
5%	0.2905	0.2080	No Confident gap	0%
10%	0.5594	0.1809	No Confident gap	0%

Finally, we have investigated the effects of uncertainty in the permittivity of the background material for the Air-Hoes 2D-PCs structure. We have considered uncertainties in ε_b of 1%, 2%, and 5% that may result from the impurities within the background material. The PDF of the bandgap and of the first and second band frequency limits are shown Figure 8 (a) and (b), respectively. The standard deviations for the PBGs for this PC structure for different tolerances of the permittivity for this case are presented in Table 6. By comparing the values of σ/Mean ratios in both Table 3 and Table 6 for the two structures of the 2D-PCs, we observe that the values of σ/Mean for the Air-Holes PCs are almost one-third there corresponding values for Si-Rods PCs structure up to uncertainty 5% in the permittivity of the Si. These

values suggest that the Air-Holes PCs could be a good candidate with least alteration in the photonic gap considering deviations that might occur in the permittivity.

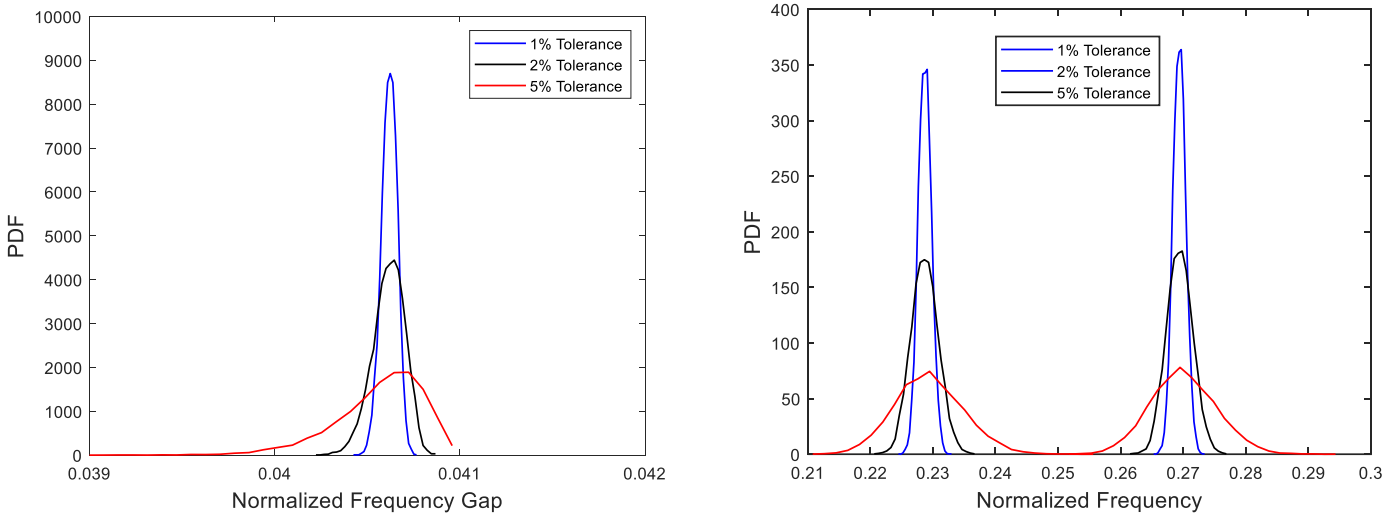

(a) **(b)**

Figure 8: (a) PDF of the normalized frequency gap for different tolerances of ε_b for Air-Holes PCs structure (b) PDF of the highest normalized frequency for the first band and the lowest Normalized frequency for the second band for different tolerances of ε_b for Air-Holes PCs structure

Table 6 : Mean and standard deviation of the normalized bandgap for different uncertainties of background's permittivity of the Air-Holes 2D PCs structure

Tolerance	Mean of the highest Normalized frequency of the first band	Mean of the lowest Normalized frequency of the second band	Mean of PBG	Standard deviation of PBG	(σ/Mean) %
1%	0.2287	0.2693	0.0406	4.3920e-05	0.108%
2%	0.2287	0.2694	0.0406	8.9293e-05	0.22%
5%	0.2290	0.2695	0.0406	2.4095e-04	0.593%

4. Conclusions

In this work, an intensive stochastic analysis for 2D-PC is presented that is based on the plane wave expansion and Monte Carlo technique. We have investigated the effects of the tolerances of the stochastic parameters of 2D-PCs on their optical operating properties. Our analysis is of great value during designing the PCs by keeping in mind the tolerances those may arise during the fabrication and their effects on the functionality of the PCs. We have examined the effects of tolerances of the stochastic parameters – the radius of the rods and the permittivities of the materials – of two-dimensional photonic crystals (2D-PCs) on their performance. In these analyses, we have studied two structures of 2D-PCs; namely Si-Rods PCs and Air-Holes PCs. Numerical results show that Si-Rods PCs structure has photonic gap that is less affected by uncertainty in radius of the rods in comparison to Air-Holes PCs structure. Our analysis revealed that the effects of uncertainty in the permittivity of Si material- up to 5%- on the photonic gap are less than those of uncertainty in dimensions for both structures. However, higher standard deviations are noticed with the Si-Rods structure in comparison with Air-Holes structure in this case.

Declarations

Funding

The authors declare that they did not receive any funding

Conflicts of interest/Competing interests

The authors declare that they have no competing interests

Availability of data and material

Not applicable

Code availability

The authors declare that they have made their custom code

Ethics approval

Not applicable

Consent to participate

Not applicable

Consent for publication

Not applicable

References

[1] O. Painter, R. K. Lee, A. Yariv, A. Scherer, J. D. O'Brien, P. D. Dapkus, and I. Kim, ''Two-dimensional photonic crystal defect laser,'' Science **284**, 1819–1821 (1999).

[2] T. Baba, N. Fukaya, and Y. Yonekura, ''Observation of light propagation in photonic crystal optical waveguides with bends,'' Electron. Lett. **35**, 654–655 (1999).

[3] Q. Gong and X. Hu, "*Photonic crystals, Principles and Applications,*" CRC Press, Taylor & Francis Group, NW (2013)

[4] J. D. Joannopoulos *et al., "Photonic Crystals: Molding the Flow of Light,"* 2nd ed, Princeton University Press, Princeton, NJ (2008).

[5] N. Susa, "Large absolute and polarization-independent photonic band gaps for various lattice structures and rod shapes," J. Appl. Phys. **91**, 3501 (2002).

[6] Y. G. Lee, "Defect modes of two-dimensional photonic crystals composed of epsilon-near-zero metamaterials," *Journal of Optics (In Press) (*https://doi.org/10.1088/2040-8986/ab7ae7)

[7] Q. Gong and X. Hu *"PHOTONIC CRYSTALS: PRINCIPLES AND APPLICATIONS,"* Pan Stanford Publishing, CRC press Taylor & Francis Group, FL (2013)

[8] C. Graham and D. Talay, “Stochastic Simulation and Monte Carlo Methods:
Mathematical Foundations of Stochastic Simulation,” *Springer Science & Business Media,* Vol. 68, 2013
[9] F. Vidal-Codina, J. Saà-Seoane, N. Nguyen and J. Peraire, “A multiscale continuous Galerkin method for stochastic simulation and robust design of photonic crystals,” *Journal of Computational Physics*: X, vol. 2, March 2019

[10] H. Zhang and S. Liu, “Analyzing the photonic band gaps in two-dimensional plasma photonic crystals with fractal Sierpinski gasket structure based on the Monte Carlo method,” AIP Advances, vol. 6, 2016.
[11] Liu, Ning, and Dean S. Oliver. "Evaluation of Monte Carlo methods for assessing uncertainty," *SPE Journal*, vol. 8, No. 2 (2003): 188-195.

[12] M. I. Wafa, Y. M. El-Batawy, S. A. El-Naggar, "Stochastic analysis for one dimensional photonic crystals," *Optik International Journal for Light and Electron Optics*, vol. 208, pp. 164106, 2020.

[13] S. A. El-Naggar, “Dependency of the photonic band gaps in two dimensional metallic photonic crystals on the shapes and orientations of rods,” *Opt. Eng.* vol. 51(6), 68001, 2012.

[14] A. H. Aly, H. A. Elsayed and S. A. El-Naggar, “The properties of cutoff frequency in two-dimensional superconductor photonic crystals,” *Journal of Modern Optics*, 61:13, pp. 1064-1068, 2014.

Figures

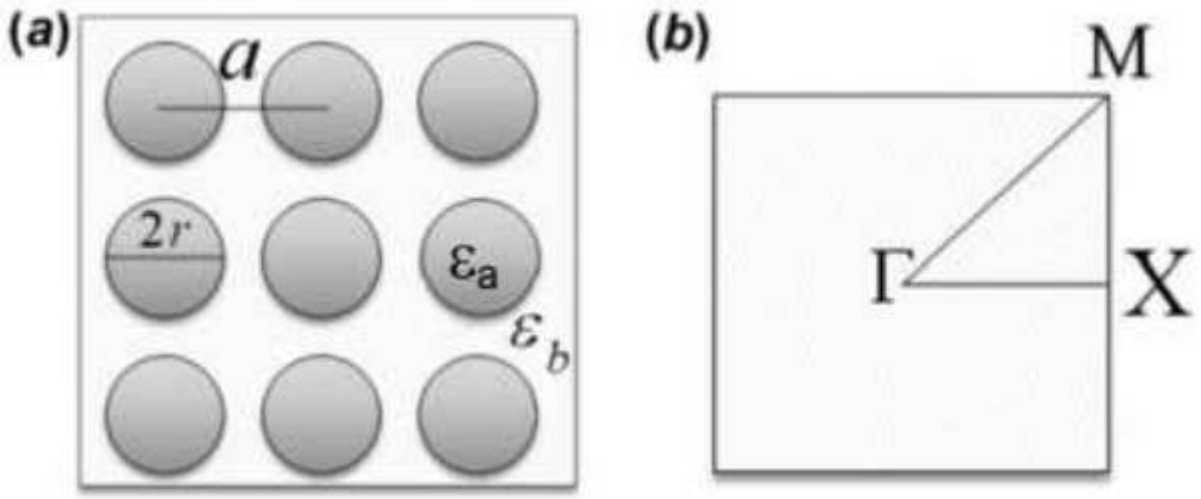

Figure 1

(a) Cross-section of 2D PCs with rods with relative permittivity of a embedded into a square lattice of background with relative permittivity of εb, (b) First Brillouin zone of the square lattice.

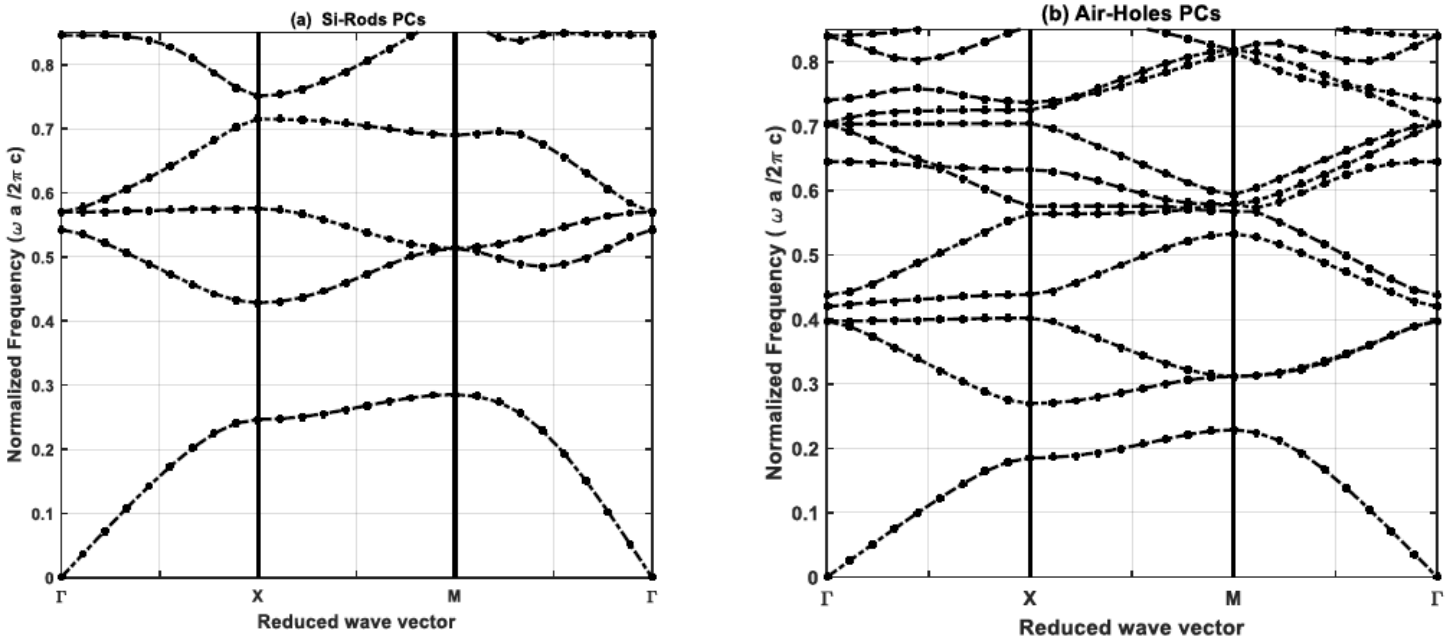

Figure 2

The photonic band structure for (a) Si-Rods PCs and (b) Air-Holes PCs.

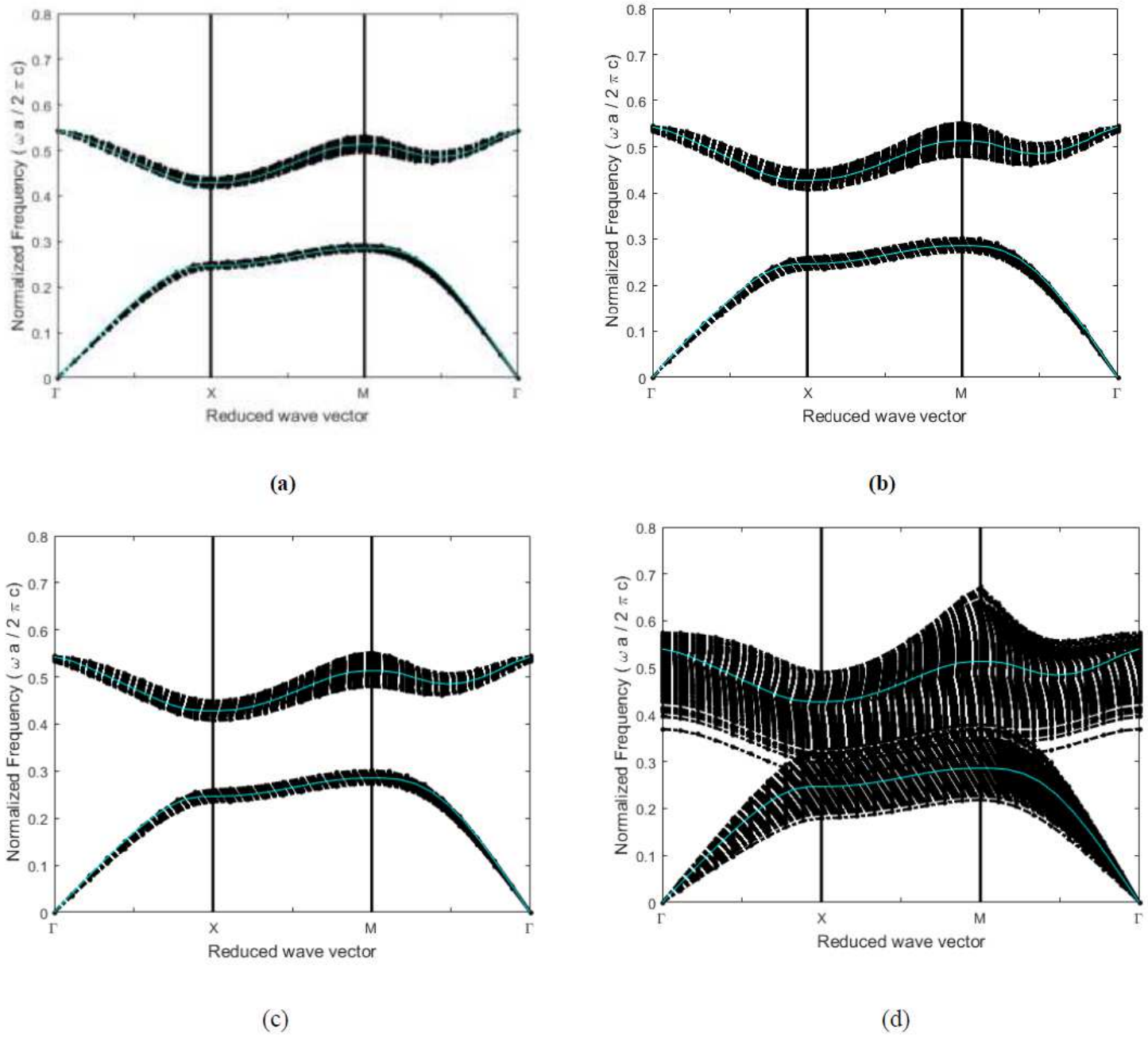

Figure 3

The Normalized frequency and Normalized frequency mean for tolerances of r and a of (a) 1%, (b) 2%, (c) 5% and (d) 10%.

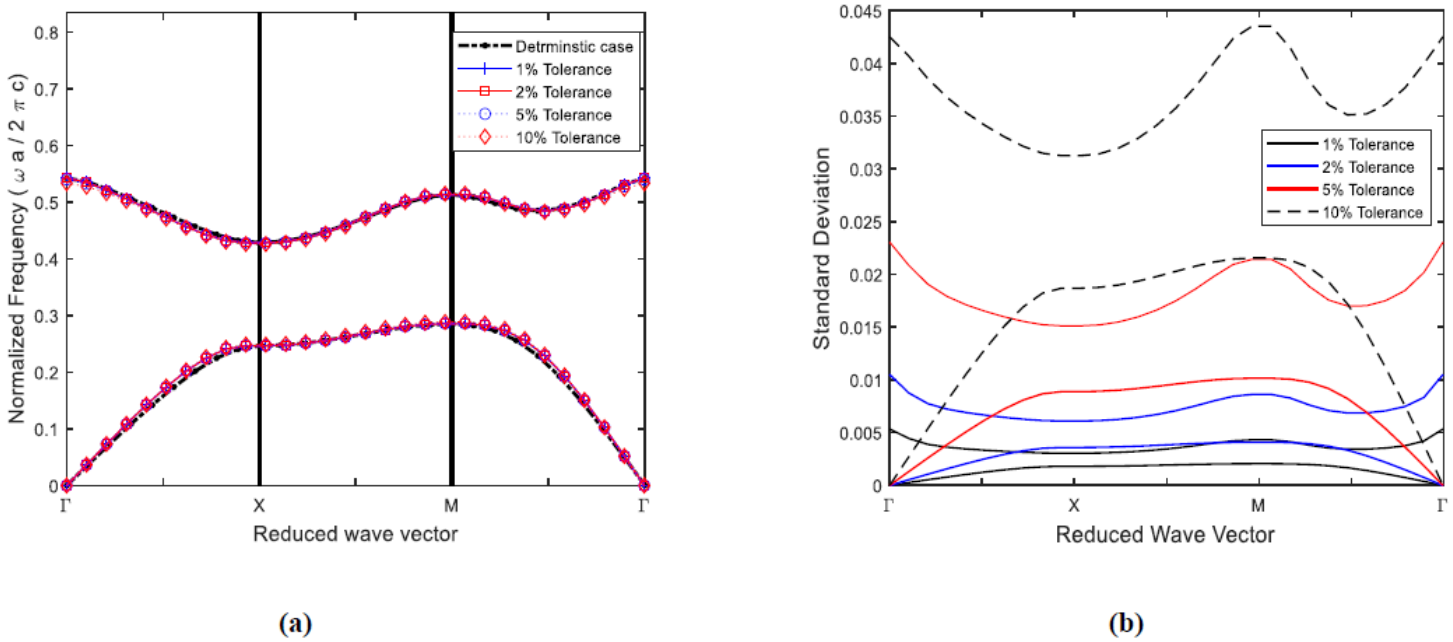

Figure 4

(a) Mean value of the band structure and the PBG vs the reduced wave vector for tolerances of 1%, 2%, 5% and 10% in both r and a. (b) Standard Deviations of both lower and upper bands of the PBG for tolerances of 1%, 2%. 5% and 10% in both r and a.

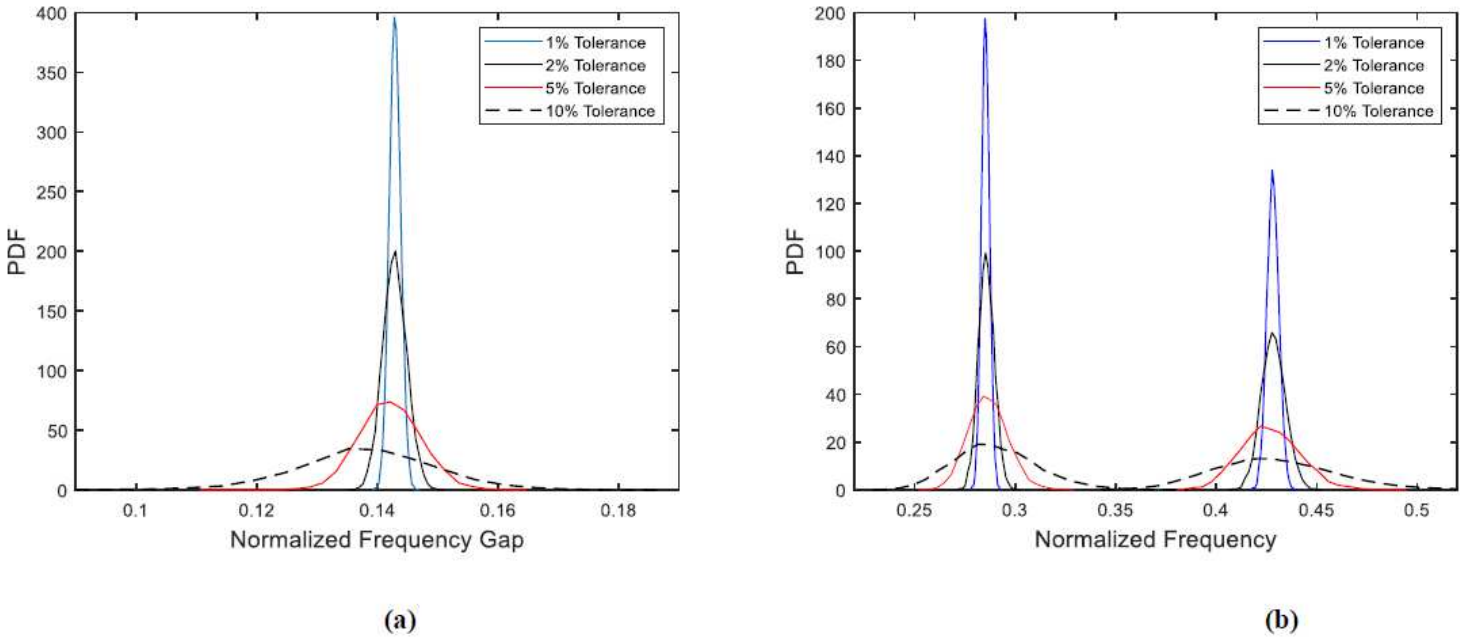

Figure 5

(a) PDF of the normalized frequency of the bandgap width for different tolerances of r and a (b) PDF of The highest normalized frequency for the first band and the lowest Normalized frequency for the second band for different tolerances of r and a

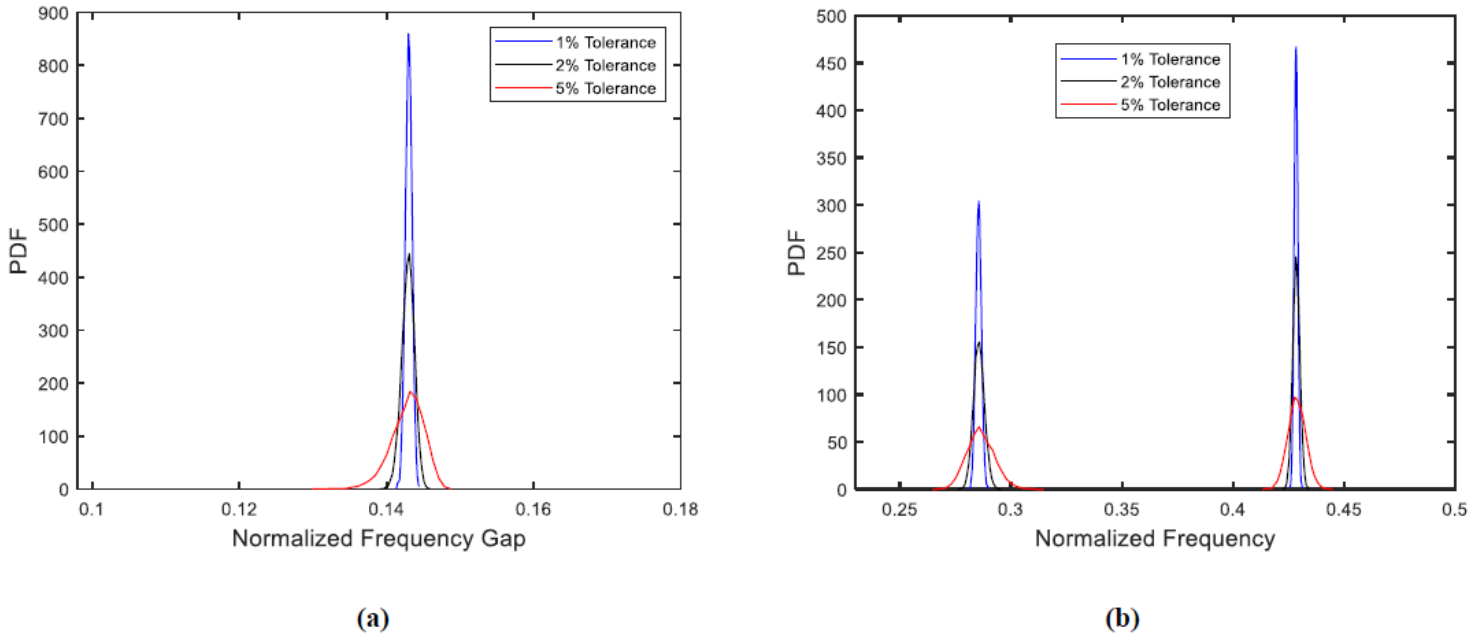

Figure 6

(a) PDF of the normalized frequency gap for different tolerances of εa (b) PDF of The highest normalized frequency for the first band and the lowest Normalized frequency for the second band for different tolerances of εa

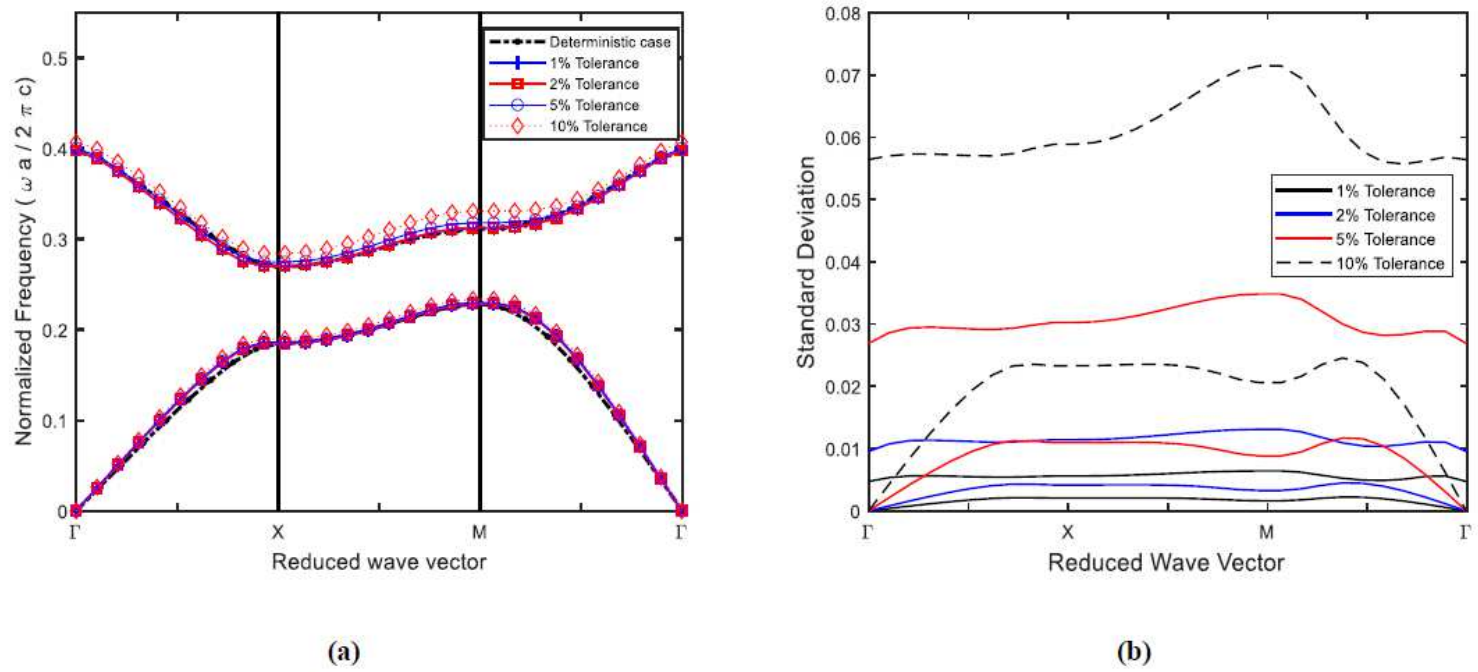

Figure 7

(a) The Mean value of the band structure and the PBG vs the reduced wave vector for tolerances of 1%, 2%, 5% and 10% in r . (b) Standard deviation of both the lower and upper bands of the PBG for tolerances of 1%, 2%. 5% and 10% in r .

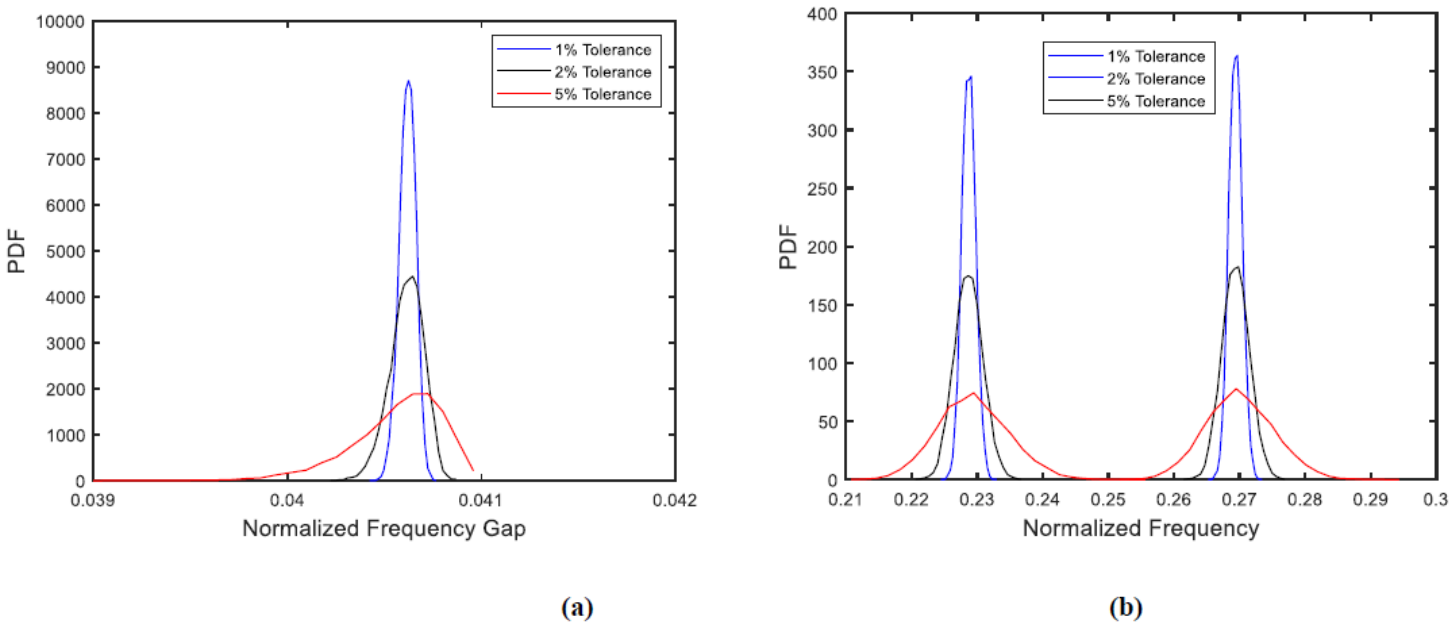

Figure 8

(a) PDF of the normalized frequency gap for different tolerances of εb for Air-Holes PCs structure (b) PDF of the highest normalized frequency for the first band and the lowest Normalized frequency for the second band for different tolerances of εb for Air-Holes PCs structure